Acta Biomaterialia 11 (2015) 393–403

Contents lists available at ScienceDirect

Acta Biomaterialia

journal homepage: www.elsevier.com/locate/actabiomat

Degradable polymer-coated gold nanoparticles for co-delivery of DNA and siRNA

Corey J. Bishop [a], Stephany Y. Tzeng [a], Jordan J. Green [a,b,c,d,*]

[a] Department of Biomedical Engineering, Translational Tissue Engineering Center, Johns Hopkins University School of Medicine, 400 North Broadway Rm 5017, Baltimore, MD 21231, USA
[b] Department of Neurosurgery, Johns Hopkins University School of Medicine, 400 North Broadway Rm 5017, Baltimore, MD 21231, USA
[c] Department of Ophthalmology, Johns Hopkins University School of Medicine, 400 North Broadway Rm 5017, Baltimore, MD 21231, USA
[d] Department of Materials Science and Engineering, Johns Hopkins University, 400 North Broadway Rm 5017, Baltimore, MD 21231, USA

ARTICLE INFO

Article history:
Received 25 June 2014
Received in revised form 20 August 2014
Accepted 12 September 2014
Available online 22 September 2014

Keywords:
Co-deliver
Gene delivery
Gold
Nanoparticle
Layer-by-layer

ABSTRACT

Gold nanoparticles have utility for in vitro, ex vivo and in vivo imaging applications as well as for serving as a scaffold for therapeutic delivery and theranostic applications. Starting with gold nanoparticles as a core, layer-by-layer degradable polymer coatings enable the simultaneous co-delivery of DNA and short interfering RNA (siRNA). To engineer release kinetics, polymers which degrade through two different mechanisms can be utilized to construct hybrid inorganic/polymeric particles. During fabrication of the nanoparticles, the zeta potential reverses upon the addition of each oppositely charged polyelectrolyte layer and the final nanoparticle size reaches approximately 200 nm in diameter. When the hybrid gold/polymer/nucleic acid nanoparticles are added to human primary brain cancer cells in vitro, they are internalizable by cells and reach the cytoplasm and nucleus as visualized by transmission electron microscopy and observed through exogenous gene expression. This nanoparticle delivery leads to both exogenous DNA expression and siRNA-mediated knockdown, with the knockdown efficacy superior to that of Lipofectamine® 2000, a commercially available transfection reagent. These gold/polymer/nucleic acid hybrid nanoparticles are an enabling theranostic platform technology capable of delivering combinations of genetic therapies to human cells.

1. Introduction

There is a need for improved nanobiotechnologies that enable intracellular delivery of difficult to deliver biologics such as nucleic acids. Ideally, a delivery material would be capable of delivering both large molecules, such as DNA, as well as small molecules, such as short interfering RNA (siRNA), and would thus be capable of both positive and negative regulation of genes. It is also necessary that such a delivery material is non-cytotoxic and desirable that it can enable multi-functionality through imaging and/or other therapeutic modalities.

Gold nanoparticles (AuNP) are easy to synthesize [1], monodisperse [1], biocompatible in various applications [2,3], have optical properties [2] useful for colorimetric sensor applications and can be diversely functionalized with chemical moieties via thiol groups [2]. They can be used as biosensors or imaging agents, and can also be used as therapeutic agents for theranostic applications. Their nanoscale size allows for the ability to passively target tumors via the enhanced permeability and retention (EPR) effect, and they can be functionalized with tumor/cancer-specific small molecules or antibodies for active targeting [4–6]. It has been shown that NPs up to 400 nm can leak through neovasculature around tumors due to abnormal endothelial cell fenestrations [7,8].

AuNPs have been imaged in vitro, ex vivo and in vivo via various modalities, either natively or with further chemical modification, such as: X-ray computed tomography, transmission electron and dark-field microscopies, multiphoton and surface-enhanced Raman spectroscopies, two-photon luminescence and photoacoustic tomography [9–11].

AuNPs are also able to be physicochemically tuned for use in photothermal therapy. When light is directed to AuNPs at the surface plasmon resonance (SPR) wavelength, heat is produced. If the nanoparticles (NPs) are engineered appropriately, cellular damage due to heat can be directed towards tumors through NP targeting and by the decreased ability of tumors to self-thermoregulate

* Corresponding author at: Department of Biomedical Engineering, Translational Tissue Engineering Center, Johns Hopkins University School of Medicine, 400 North Broadway Rm 5017, Baltimore, MD 21231, USA. Tel.: +1 410 614 9113; fax: +1 443 287 6298.
E-mail address: green@jhu.edu (J.J. Green).

http://dx.doi.org/10.1016/j.actbio.2014.09.020
1742-7061/

[12]. SPR wavelengths may be tuned in the near-infrared (NIR) region, which is useful as NIR is transparent to biological tissue on the order of centimeters [13].

AuNPs are able to deliver a payload through conjugation or ionic complexation to small molecules [14] or various nucleic acids, such as DNA [15], short hairpin RNA and siRNA [16], for promoting or inhibiting protein expression. Layer-by-layer (LbL) approaches coat a surface or a core with multiple layers of charge-alternating polyelectrolytes [15,17–21]. NP LbL approaches are ideal for complexing ionically charged macromolecules into EPR-relevant sizes. LbL approaches can be accomplished using aqueous solvents, are versatile regarding molecular structure as natural and synthetic polyelectrolytes can be used, and are easily tuned by varying the number and order of the layers [18,22].

Although viruses may be effective nucleic acid delivery vectors, many have been associated with immune complications and/or insertional mutagenesis and therefore we have focused our efforts on safer, non-viral methods [23]. In this work, we report a proof of concept of simultaneous non-viral knockdown and exogenous gene expression via an LbL theranostic platform technology with biodegradable polymers as outer layers. This system was validated in vitro using human primary glioblastoma multiforme (GBM) cells [24,25]. The hybrid NPs employ two uniquely degrading polymers for release – one based on the hydrolysis of ester groups and the other based on environmentally triggered degradation of disulfide linkages once the particles are in the cytoplasm. The ability to simultaneously inhibit and generate proteins of interest with these NPs has many applications in cancer therapeutics, such as overcoming drug resistance, promoting apoptosis and inhibiting migration, as well as rectifying diseases caused by aberrant proteins [26,27].

2. Materials and methods

2.1. Materials

The AuNPs were synthesized using tetrachloroauric acid ($HAuCl_4$) trihydrate (Ted Pella, Inc.), sodium citrate (Na_3-citrate) tribasic dehydrate (Sigma Aldrich), a reflux condenser (Sigma Aldrich), mineral oil (Sigma Aldrich), a hot plate with magnetic stir bar (Fisher Scientific) and 11-mercaptoundecanoic acid (11-MUA). The polymers were synthesized from commercially available monomers N,N′-bis(acryloyl)cystamine (BSS; Alfa Aesar), 3-amino-1-propanol (S3; Alfa Aesar), 1-(3-aminopropyl)-4-methylpiperazine (E7; Alfa Aesar), 1,4-butanediol diacrylate (B4; Alfa Aesar) and 4-amino-1-butanol (S4; Alfa Aesar). Other reagents used included sodium acetate (NaAc), ethanol (EtOH), anhydrous dimethyl sulfoxide (DMSO; Sigma Aldrich), methanol (MeOH; Sigma Aldrich), 25 kDa branched polyethyleneimine (Sigma Aldrich), anhydrous tetrahydrofuran (THF; Sigma Aldrich), anhydrous ethyl ether (Fisher Scientific), Lipofectamine® 2000 (Invitrogen), OptiMEM I (Invitrogen), YO-PRO®-1 (Y3603; Invitrogen), Picogreen® (P7589; Invitrogen), Ribogreen® (Q10213; Invitrogen) and Fluoraldehyde™ OPA assay (26025; Thermo Scientific). Cell culturing reagents included: fetal bovine serum (FBS), DMEM:-Ham's F12 (1:1) (Invitrogen), 1× antibiotic–antimycotic (Invitrogen), anti-eGFP siRNA (sense: 5′-CAAGCUGACCCUGAAGUUCTT; anti-sense: 3′-GAACUUCAGGGUCAGCUUGCC), scrambled siRNA as a negative control (sense: 5′-AGUACUGCUUACGAUACGGTT; anti-sense: 3′-CCGUAUCGUAAGCAGUACUTT), plasmid-enhanced green fluorescent protein DNA (eGFP-N1; referred to as eGFP) (Clontech), amplified and purified by Aldevron, pDsRed-Max-N1 DNA (dsRed) (Addgene) and CellTiter 96® AQueous One Solution Cell Proliferation Assay (Promega).

2.2. Colloidal AuNP synthesis

Similar to the Frens method [1], 1 ml of a 1% solution of Na_3-citrate was quickly injected into 20 ml of a 0.01% solution of $HAuCl_4$ that was vigorously boiling in a round bottom flask using mineral oil, a hot plate with magnetic stirring capabilities and a reflux condenser, and boiled for an additional 6 min. As the nucleation and growth of the AuNPs proceeded, the solution turned from a slightly yellow color to deep red. After boiling, the citrate-stabilized AuNPs (CAu) were cooled on ice for approximately 10 min. 11-MUA was conjugated to the AuNPs (MAu) to help ensure charge stability throughout the layering process. To do so, a 20 mM solution of 11-MUA was made in 95% EtOH and diluted to 1 mM using 70% EtOH, which had been diluted from 95% using 150 mM NaAc. The CAu was centrifuged at 20 kRCF for 10 min and, after the supernatant was removed, an equal amount of the 1 mM 11-MUA solution was used to resuspend the CAu. The solution was sonicated at an amplitude of 1 for 2 s using a Misonix Ultrasonic Liquid Processor. The conjugation took place over 48 hours at room temperature and sonicated at approximately 4 and 40 h during the conjugation process. The solution was washed in water twice by centrifugation (21 kRCF for 10 min) and became deep purple and cloudy with sonication as the 11-MUA crashed out of solution in the water. The solution was then washed twice in ethanol and twice more in 4.5 mg ml^{-1} Na_3-citrate via centrifugation (21 kRCF for 10 min). The solution retained its purple hue but was no longer cloudy. The resulting MAu solution in 4.5 mg ml^{-1} Na_3-citrate was stable. The MAu solution was diluted to 0.31 nM and used in the LbL process.

2.3. CAu and MAu physical characterization

Transmission electron microscopy (TEM; Philips/FEI BioTwin CM120) was used to ascertain the diameter of the AuNPs on carbon-coated copper grids (FCF400-Cu; Electron Microscopy Sciences), which was then used to calculate the extinction coefficient ε according to Liu et al. according to Eq. (1) [38]:

$$\ln \varepsilon = 3.32111 \ln \text{Diameter}_{\text{AuNP in nm}} + 10.80505 \quad (1)$$

The concentration was determined by dividing the normalized absorbance (A cm^{-1}), which was measured using ultraviolet–visible (UV–Vis) spectroscopy (Synergy2, Biotek®, Gen5 software), by ε according to the Beer–Lambert law. The aggregation differences of naked CAu and MAu were assessed by their placement into increasingly more concentrated solutions of sodium acetate, which was the buffer used for layering (pH 5.2). The final concentration of sodium acetate after the first layer (poly(ethylenimine), PEI) was added to the AuNPs was 63 mM.

2.4. Polymer synthesis and characterization

The reducible disulfide-containing poly(amido amine) (BSS–S3–E7 or SS37) [39–41] and the hydrolytically degradable poly(beta-amino ester) (B4–S4–E7 or 447) [24] polymers were synthesized as previously reported (Scheme S1).

Briefly, polymer SS37 was synthesized by adding the BSS monomer in a 4:1 v/v mixture of MeOH and water, and subsequently adding the S3 monomer in a 1.05:1 M ratio under nitrogen. The reaction was kept in the dark, with constant stirring under positive nitrogen pressure via a balloon syringe at 45 °C for 14 days (Scheme S1). The solution became clear after the first couple of hours. Once the reaction was complete, the polymer was purified using reverse dialysis with a molecular weight cut-off of 2 kDa in 2 l of pH 3 Milli-Q water with constant stirring for 24 h. The pH 3 water was replaced at 8 h. After washing in water using centrifugation, the polymer was frozen in liquid nitrogen and lyophilized.

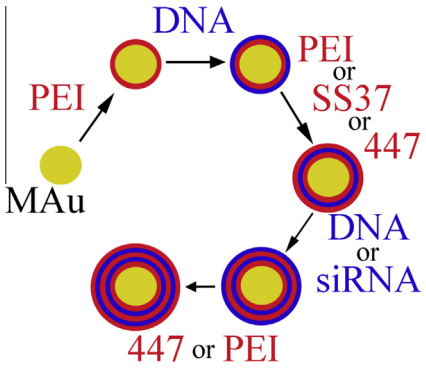

Scheme 1. LbL process starting with MAu.

The polymer was then made into a 167 mg ml^{-1} solution using anhydrous DMSO. Next, 0.5 M E7 in DMSO was added to dilute the 167 mg ml^{-1} solution to 100 mg ml^{-1}.

Polymer 447 was synthesized by mixing neat monomers B4 and S4 in a 1.2:1 M ratio. The reaction was carried out for 24 h at 90 °C in the dark with constant stirring. The diacrylate-terminated base polymer was dissolved in anhydrous THF. E7 in anhydrous THF was added for a final concentration of 100 mg ml^{-1} B4–S4 base polymer and 0.2 M E7 endcap, and the mixture was left to react for 1 h while shaking at 1000 rpm (Scheme 1). The endcapped polymer was then precipitated into anhydrous ethyl ether in a 4:1 v/v ratio of ether to THF. The polymer was collected by centrifugation at 4000 rpm for 5 min, the supernatant was decanted, and the polymer was washed once more with ether and collected by centrifugation. Polymer was allowed to dry for 2 days under vacuum, then dissolved in anhydrous DMSO at a final polymer concentration of 100 mg ml^{-1} and subsequently stored at −20 °C with desiccant until use.

Gel permeation chromatography (GPC) (Waters,® Breeze 2 software) was used to assess the number average molecular weight (M_n), weight average molecular weight (M_w) and polydispersity index using three 37.8 × 300 mm columns in series at a flow rate of 1 ml min^{-1} of GPC solvent (94% THF, 5% DMSO and 1% piperidine, containing approximately 10 mg of butylated hydroxytoluene).

2.5. Polyelectrolyte layering process

The layering process is depicted in Scheme 1 [18,22]. In the process, 80 µl of 25 kDa branched PEI was added to 112 µl of the 0.31 nM MAu (1.9 × 10^{11} particles ml^{-1}) in water, which was shaken for 30 min at 500 rpm at room temperature and centrifuged twice at 10 kRCF for 10 min to remove uncomplexed polyelectrolytes (extracted 182 µl). The supernatant was replaced after the first and second washings with 182 and 102 µl of 150 mM NaAc, respectively. Each subsequent layer was added to the previous resuspended complexes using 80 µl of the polyelectrolyte in 150 mM NaAc. The order in which the polyelectrolytes were layered with their associated concentrations are as follows: MAu (0.31 nM)–PEI (10 mg ml^{-1})–DNA (0.5 mg ml^{-1})–PEI (10 mg ml^{-1}) or SS37 (5 mg ml^{-1}) or 447 (5 mg ml^{-1})–DNA (0.5 mg ml^{-1}) or anti-eGFP siRNA (4 µM)–447 (1.25, 2.5 or 5 mg ml^{-1}) or PEI (0.25 mg ml^{-1}). The supernatant of the second wash was replaced with 25 mM NaAc just prior to the addition of the last layer, and the last polyelectrolyte layer was also added in 25 mM NaAc.

2.6. Diameter and zeta potential

The diameter and zeta potential (ZP) at each of the layered stages of the DNA/siRNA co-delivery NP formulation with a 447 concentration of 5 mg ml^{-1} were ascertained via NP tracking analysis using a NanoSight NS500 ($n \geqslant 2$), and a Malvern Zetasizer Nano ZS (Smoluchowski model, Malvern Instruments; detection angle 173°, 633 nm laser) ($n = 3$), respectively. The diameters were calculated after the two washing steps just prior to adding the subsequent layer in the same diluent (0- to 3.1-fold dilution), as in the usual polyelectrolyte layering process. The unknown diffusivity (D) was calculated from the root mean square distance ($\langle x \rangle$) and time (t) in Eq. (2) (two-dimensional) below:

$$\langle x \rangle = \sqrt{4Dt} \tag{2}$$

which can then be used to calculate the unknown hydrodynamic radius using the Stokes–Einstein equation shown in Eq. (3):

$$D = \frac{K_B T}{6\pi\mu r} \tag{3}$$

where K_B is the Boltzmann constant, T is the temperature (in kelvin), μ is the viscosity and r is the hydrodynamic radius. The ZPs were measured after the second washing at each layer after a 3.6-fold dilution in ultrapure distilled water.

Although the diameter quantified using the NanoSight NS500 instrument is also an indicator of aggregation, we endeavored to corroborate these findings via TEM. In doing so, 30 µl of the sample of interest was placed onto corona plasma-treated, carbon-coated copper grids. CAu in water was air dried; the PEI-to-447 layers (using the 11-MUA conjugated CAu or MAu) layers were adsorbed for 30–45 min, followed by wicking and rinsing in water. Similar to when the diameter and ZP were assessed, the 447 layer was at 5 mg ml^{-1}.

2.7. Nucleic acid loading and layering efficiency

To quantify the amount of nucleic acid loaded in the various formulations, three different nucleic acid-intercalating probes were used. When quantifying the amount of DNA in the absence of siRNA, YO-PRO®-1 was used. YO-PRO®-1 can fluoresce in the presence of either DNA or siRNA; therefore, nucleic acid-specific intercalating probes were used when quantifying DNA and siRNA in the presence of the other – namely, Picogreen® and Ribogreen®, respectively.

When quantifying the amount of nucleic acid present using DNA intercalators, it is important to ensure that all of the ionically complexed nucleic acid is detected as the complexed form is less accessible to the nucleic acid-intercalating probes. To ensure that all the nucleic acid present was detected in the presence of polymer, branched PEI with a known amount of DNA or siRNA using 10 weight/weight (w/w; mass ratio of polymer to nucleic acid) was used for optimization of the disassembly process ($n \geqslant 3$) by adjusting the salt and heparin concentrations. When quantifying the amount of DNA in the absence of siRNA, the formulation is brought to 10 µM YO-PRO®-1, 650 mM salt (phosphate buffered saline (PBS) and NaAc) and 300 µg ml^{-1} of heparin, and measured using a fluorescence plate reader (excitation and emission of 485 and 528 nm, respectively). When quantifying the amount of DNA in the presence of siRNA, the formulation tested is brought to 650 mM salt (PBS and NaAc) and 110 µg ml^{-1} of heparin at the completion of the layering process, and measured using a 1:200 dilution of Picogreen® in a 1× Tris and EDTA (TE) buffer using excitation and emission of 485 and 528 nm, respectively (1 µl of sample + 199 µl of 1:200 dilution Picogreen® in 1× TE buffer). When quantifying siRNA in the presence of DNA, the formulation is brought to 8 mM salt (PBS and NaAc) and 1040 µg ml^{-1} heparin, and measured using a 1:200 dilution of Ribogreen® in the provided RNA BR buffer using excitation and emission of 644 and 673 nm, respectively (10 µl of sample + 200 µl of 1:200 dilution Ribogreen® in RNA BR buffer). The co-delivery DNA/siRNA LbL formulation's

DNA and siRNA content was quantified after adding polymer 447 at 5 mg ml^{-1} (highest w/w formulation). The same DNA and siRNA content was used to calculate the w/w values when 2.5 or 1.25 mg ml^{-1} polymer 447 was added as the last layer, as there is the same amount of nucleic acid present before the 447 polymer is complexed (Table S1).

The content of DNA and siRNA in the supernatants during the washing steps was quantified with a NanoDrop 2000 Spectrophotometer (Thermo Scientific). The layering efficiency was calculated by multiplying the amount of nucleic acid ionically complexed per vial by 100 and dividing by the total amount of nucleic acid added per vial.

2.8. Weight/weight

The w/w values for the layered formulations were calculated by dividing the mass of the unwashed polymer on the outer layer of the various formulations per mass of DNA or siRNA loaded per vial. Although the majority of the polymer in the layered formulations is the unwashed outer layer, we investigated the extent to which an earlier washed polymer layer could be contributing to the w/w values. The amount of PEI complexed was calculated by subtracting the uncomplexed PEI extracted in the supernatants from the amount of PEI added. This was calculated using a Fluoraldehyde™ OPA assay, which detects primary amines using excitation and emission of 340 and 420 nm, respectively.

2.9. Cell culture and transfection

The human glioblastoma multiforme cell line (GBM319) was derived from brain tumor stem cells (from a 79 year old patient) and cultured as previously described [25] in a humid 37 °C and 5% CO_2 atmosphere using DMEM:Ham's F12 (1:1), supplemented with 1× antibiotic–antimycotic (Invitrogen) and 10% FBS. These eGFP-negative cells were used to assess expression in layered formulations delivering DNA only (eGFP). To assess the ability to co-deliver DNA and siRNA using layered formulations (termed LD or HD; see Section 3.3 for definitions), stably expressing eGFP-positive GBM319 cells were used which were previously transfected with B4-S5-E3/eGFP polyplex and retained eGFP positivity in 1.2% of the cells 3 months post-transfection [42]; these cells were sorted via fluorescence activated cell sorting multiple times to obtain a more pure eGFP-positive population of 81%. Knockdown in the stably expressing eGFP-positive GBM319 cells was assessed using anti-eGFP siRNA and a scrambled siRNA as a control. Expression in the stably expressing eGFP-positive cells was assessed using red fluorescence protein transcribed and translated from dsRed DNA. Lipofectamine® 2000 was used as a positive control for knockdown and expression. All formulations were delivered as 20 μl, except for Lipofectamine® 2000 delivering dsRed DNA.

The GBM319 cells (eGFP-positive and negative) were seeded in 96-well plates at 10,000 cells well^{-1} 1 day prior to transfection. The positive controls and various layered formulations were delivered to the cells and the 96-well plates were gently rocked manually. The medium was changed 2 h after delivery.

2.10. Transfection assessment and quantification

Fluorescence microscope images (Zeiss) were taken of the various formulations on days 1–3 (10× magnification) for expression and day 7 (5× magnification) for knockdown. The exposure times for the eGFP and dsRed channels were 200 and 600 ms, respectively.

A Synergy2 fluorescence plate reader was used to assess knockdown each day until the strongest knockdown reached a maximum, whereupon the knockdown was assessed using the more sensitive method of flow cytometry. To ensure that the knockdown assessment is due solely to RNA interference and is not a result of cytotoxicity, a scrambled control was used. The knockdown was calculated using Eq. (4) using excitation and emission of 485 and 528 nm:

$$Knockdown\% = 100\left(1 - \frac{[F_{si} - F_{Background}]}{F_{osi}}\frac{F_{osc}}{[F_{sc} - F_{Background}]}\right) \quad (4)$$

where F_{si} is the fluorescence of the well using anti-eGFP siRNA, F_{sc} is the fluorescence of the well using scrambled siRNA, $F_{Background}$ is the fluorescence background of the medium without cells, F_{osi} is the initial fluorescence of the well just prior to delivery for the anti-eGFP formulations and F_{osc} is the initial fluorescence of the well just prior to delivery for the scrambled siRNA formulations.

ImageJ analysis was performed on days 1–3 to determine the day of maximal expression. A BD Accuri™ C6 flow cytometer equipped with an automatic HyperCyt sampler was used to assess expression at day 2 and knockdown at day 7. The singlet population was identified using FSC-H vs. SSC-H; the FL1-H vs. FL3-H channel was used to assess the eGFP and dsRed population percentages. When the stably expressing eGFP GBM319 cells were used to assess co-delivery of DNA and siRNA, an FL1 90% filter was used to ensure that the FL1 detector was not saturated. FL1-H vs. FL3-H was chosen as this minimizes the overlapping fluorescence. Knockdown was calculated by flow cytometry, by quantifying the geometric mean for the anti-eGFP siRNA and scrambled groups of the eGFP-positive region using FL1-A, according to Eq. (5):

$$Knockdown\% = 100 - 100\frac{\text{anti-eGFP siRNA Geometric Mean}}{\text{scrambled siRNA Geometric Mean}} \quad (5)$$

2.11. Cytotoxicity

An MTS assay, CellTiter 96®, was used to assess the relative metabolic activity (RMA) relative to an untreated group, which was normalized to 100% 24 h post-transfection. The MTS assay is an indicator of cytotoxicity or viability. We wished to evaluate if the nanoparticles became increasingly cytotoxic following the degradation of the outer layer, which was composed of biodegradable polymer 447. This polymer has been shown to have a half-life of 2–5 h [31]. We therefore incubated the particles at 37 °C in complete medium for 18 h and then added them to GBM319 cells at the same concentration and dosage as the HD5 formulation. Cellular viability was measured using an MTS assay at 24 h post-transfection. A two-tailed Student's *t*-test was used to compare the degraded and non-degraded HD5 formulations.

2.12. Cellular uptake

TEM was also used to assess cellular uptake of the co-delivery LbL formulation. The GBM319 cells, after 2 h of LbL formulation incubation using the 300 ng DNA and 240 ng of siRNA formulation at respective w/w values of 56 and 69, were fixed, dehydrated and infiltrated with Epon, then sectioned into 70–100 nm slices using an ultramicrotome.

More specifically, the cells were washed with PBS and were fixed using a glutaraldehyde buffer (2.5 vol.%; 0.1 M sodium cacodylate buffer (CaCO), 3 mM CaCl, 1% sucrose, pH 7.2–7.4) and rocked overnight at 4 °C. The following day, the cells were washed 3× in a new glutaraldehyde buffer (0.1 M CaCO, 3 mM CaCl, 3% sucrose) for 15 min each, while making sure that the cells did not dry out. The cells were then left in the dark with a 1% osmium tetroxide solution (0.1 M CaCO, 3 mM CaCl) for at least 1 h on ice before being washed twice in fresh deionized water for 5 min. Filtered (0.22 μm) 2% uranyl acetate solution in water was used to cover the cells for a maximum of 1 h in the dark. The cells then

underwent a dehydration series using 50, 70, 90 and 100% ethanol (freshly opened). Subsequently, Epon (1:1 solution of propylene oxide:Epon) was added in a swirling fashion and left overnight. The following day, Epon with 1.5% DMP-30 (Ted Pella, Inc.) catalyst was added and placed in a vacuum chamber (15 inches of Hg) for 2 h twice and then placed on a rocker for another 2 h. The Epon was again replaced and put into an oven at 37 °C, where it was allowed to cure for 72 h. The cells were then placed at 60 °C for 24 h. Pliers were used to break the edges carefully, then the dish was snapped off to allow clean breaks and to minimize the creation of aberrant lines in the sample. The samples were cut out and sliced using an ultramicrotome and imaged on formvar-coated notched grids (Electron Microscopy Sciences).

2.13. Statistics

All errors reported are standard error of the means. The errors reported in Fig. 1B ($n = 3$) and 2A ($n \geqslant 2$) are independently prepared samples with at least three technical replicates (TR), except CAu and Mau, which are TR ($n = 3$) as they are from a single batch synthesis. The errors in Fig. S3 are TR ($n \geqslant 3$). The errors reported in Table 1 and Fig. S4 are $n \geqslant 3$ with at least 3 TR. Fig. 3 errors are TR (LD and HD, $n = 20$; Lipofectamine® 2000, $n = 4$); a one-way analysis of variance (ANOVA) was performed using a Bonferroni's multiple comparison test to assess knockdown differences between the day of maximum knockdown and day 7, when flow cytometry was performed (a p-value of >0.05 is not significant). Errors reported in Fig. 4 are TR (LD, HD and untreated are $n \geqslant 16$; Lipofectamine® 2000 is $n = 4$); a one-way ANOVA was performed using a Bonferroni's multiple comparison test post hoc, where *** is a p-value of <0.0001. Figs. S6, S7 and S9 are TR with $n = 4$, $n \geqslant 4$ and $n \geqslant 4$, respectively. A one-way ANOVA was performed in Fig. 7 and S9 using a Dunnett's multiple comparison test to assess significance between Lipofectamine® 2000, where *** is a p-value of <0.0001.

3. Results

3.1. CAu and MAu physical characterization

CAu batches were synthesized following a modified Frens method [1] (see Methods). CAu NPs were then conjugated with 11-MUA to obtain MAu NPs that were 17 ± 2 nm in diameter (Fig. 1; far left). Based on the TEM diameter of the CAu, the extinction coefficient, ε, was calculated to be 6.3×10^8 M^{-1} cm^{-1}. Using the absorbance from UV–Vis spectrometry, the working concentration of MAu was calculated to be 0.31 nM, which is equivalent to 1.9×10^{11} particles ml^{-1}. The SPR wavelength of the 11-MUA-unconjugated CAu was 520 nm in 4.5 mg ml^{-1} Na_3-citrate (pH 7.1) and was red-shifted to 526 nm after 11-MUA conjugation (Fig. S1), indicating that the 11-MUA was conjugated successfully.

Table 1
Nucleic acid dosages and mass ratio of the 447 polymer to DNA (w/w) values of the various layered formulations.

Formulation	DNA (ng)	Mass ratio (w/w)
MAu-P-D	980 ± 30	0
MAu-P-D-P	1050 ± 30	79
MAu-P-D-447	950 ± 50	44
MAu-P-D-P-D-447	2400 ± 100	17
MAu-P-D-447-D-447	510 ± 20	82
MAu-P-D-SS37-D-447	450 ± 40	92
LD and HD	See Section 3.6 and Table S1	See Section 3.6 and Table S1

The w/w values are calculated from the most outer layer of polymer as described in Section 3.6.

The MAu solution aggregated far less than the CAu solution, as indicated by the degree to which the SPR wavelengths red-shifted when placed in acidic NaAc buffer (Fig. S2).

3.2. Polymer characterization via gel permeation chromatography

1-(3-Aminopropyl)-4-methylpiperazine end-modified poly(N,N′-bis(acryloyl)cystamine-co-3-amino-1-propanol) (abbreviated here as SS37) contained disulfide bonds. The 1-(3-aminopropyl)-4-methylpiperazine end-modified poly(1,4-butanediol diacrylate-co-4-amino-1-butanol) (abbreviated here as 447) is a poly(beta-amino ester) (PBAE) containing ester linkages.

Polymer molecular weight was ascertained by GPC. SS37 had an M_n and M_w of 2.5 and 2.7 kDa, respectively. 447 had an M_n of 10.2 kDa and an M_w of 39.8 kDa.

3.3. LbL notation

Throughout the paper the notation to describe layered NPs is as follows: PEI is abbreviated as "P", DNA as "D", and the synthetic polymers as "SS37" and "447". The specific mutilayered formulation that contains DNA and siRNA, MAu-P-D-SS37-siRNA-447, is referred to as "LD" or "HD", corresponding to low nucleic acid dose (LD) or high nucleic acid dose (HD). We investigated six different co-delivery multilayer particle formulations: two nucleic acid dosages at three different 447 concentrations (1.25, 2.5 or 5 mg ml^{-1}) as the last layer. These formulations are referred to as the low (LD) or high dosage (HD), following by 1.25, 2.5 or 5 mg ml^{-1} to indicate the polymer concentration of the last layer (e.g. "LD2.5" or "HD5").

3.4. Diameter and zeta potential

By dynamic light scattering (DLS; Malvern Zetasizer) the measured intensity-weighted diameters for CAu and MAu were 23 ± 1 and 27 ± 2 nm, respectively. NanoSight calculated the concentration of layered particles for the HD5 formulation (MAu-P-D-SS37-siRNA-447) to be $(2.6 \pm 0.5) \times 10^9$ particles per ml. The

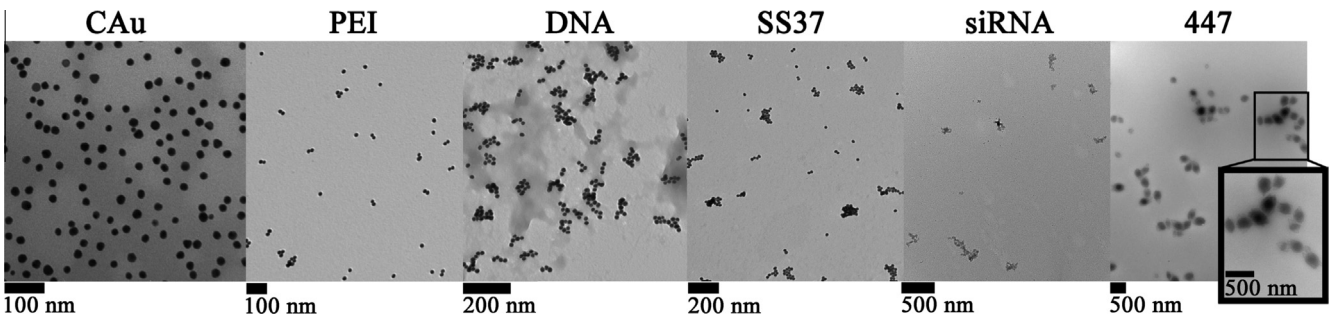

Fig. 1. TEM images of each of the layered stages showing nanoparticle size. The addition of the DNA layer results in the initial clustering together of multiple gold nanoparticle cores to form a single particle.

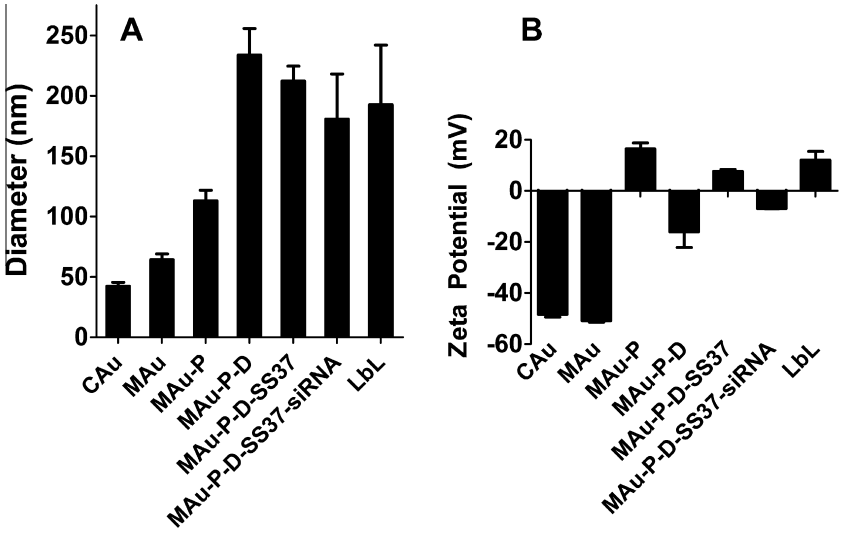

Fig. 2. Diameter (A) and ZP (B) at each of the layering stages.

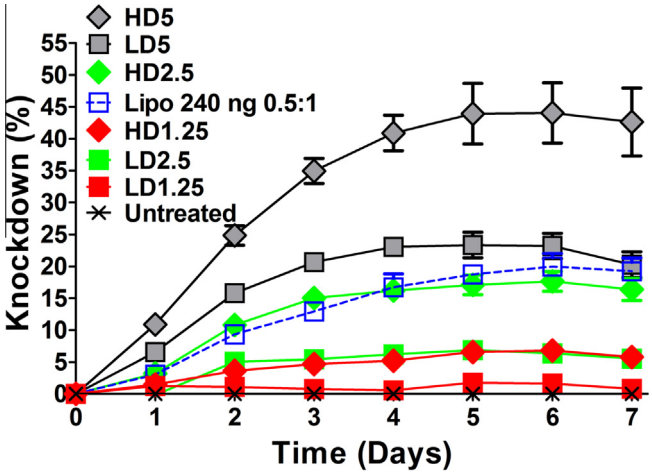

Fig. 3. SiRNA-mediated knockdown over time of GFP in human brain cancer cells resulting from delivery of MAu/DNA/siRNA LbL particles. The nanoparticle dosages and amount of 447 polymer in the outer layer were varied. Optimized particles had higher knockdown than the optimized formulation of the leading commercially available reagent Lipofectamine® 2000.

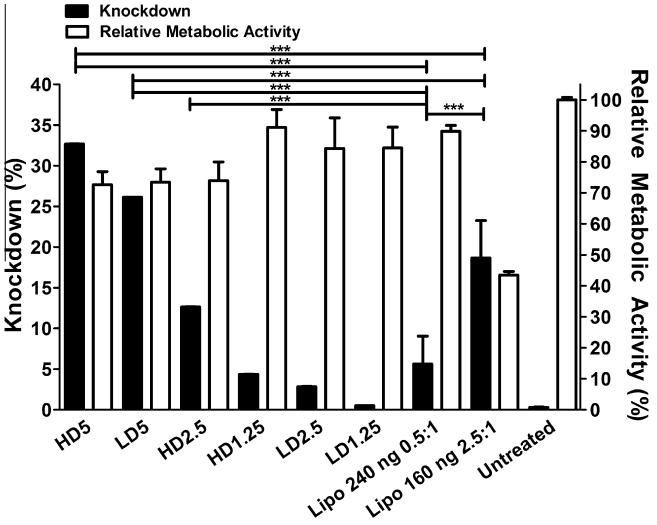

Fig. 4. SiRNA-mediated knockdown of MAu/DNA/siRNA LbL particles on day 7 and relative metabolic activity at 24 h post-transfection of LbL NPs.

largest increase in size following layering was observed when transitioning from MAu-P to MAu-P-D, when the DNA was added, leading to AuNP clusters consisting of several AuNPs within each larger particle of approximately 230 nm (Fig. 2A). Despite using higher concentrations of DNA (0.75 and 1.0 mg ml^{-1}), the diameter of the MAu-P-D formulation was not able to be decreased significantly. The diameters of the MAu-P-D formulation using 0.75 and 1.0 mg ml^{-1} were 180 ± 10 nm ($n = 3$; $p = 0.20$) and 170 ± 10 nm ($n = 3$; $p = 0.18$). As each subsequent polyelectrolyte layer was added to the NPs and washed, the ZP of the NPs reversed in charge (Fig. 2B).

TEM indicated a progressive increase in size up to the DNA layer. At this layer, TEM showed clustering of AuNPs into larger nanoparticles (Fig. 1).

3.5. Nucleic acid loading and layering efficiency

Nucleic acid loading and layering efficiency was determined through evaluation with nucleic acid binding dyes. For measurements, heparin and salt concentrations (PBS and NaAc) were optimized to displace polymer and allow the intercalating fluorescence dyes to detect the total nucleic acid present in the presence of 25 kDa PEI at 10 w/w. YO-PRO®-1, Picogreen and Ribogreen were able to detect 94.8 ± 0.8, 101 ± 2 and 100 ± 2%, respectively, of the nucleic acid present (Fig. S3). The amount of nucleic acid delivered per 96-well plate well in 20 µl volumes for the layered formulations is shown in Table 1 (w/w discussed in Section 3.6). The DNA doses delivered by the layered formulations ranged from 200 to 2400 ng and the siRNA doses ranged from 160 and 240 ng siRNA.

In contrast to the MAu-P-D-P-D-447 formulation, the loading of the MAu-P-D-447-D-447 and MAu-P-D-SS37-D-447 formulations were determined to have lower loading than would be otherwise anticipated based on the loading of the MAu-P-D formulation. We observed that DNA loading was at a maximum when only non-degradable, highly charged polymers were used in the middle layers of the formulation, rather than more weakly charged and biodegradable polymers. This loading difference may be due to the differences in binding affinity between the various cationic polymers and DNA [24,28].

When one DNA layer was utilized, the average percentage of nucleic acid retained in the layering process (i.e. the layering efficiency) was 24.1 ± 0.4%. When either SS37 or 447 polymer was

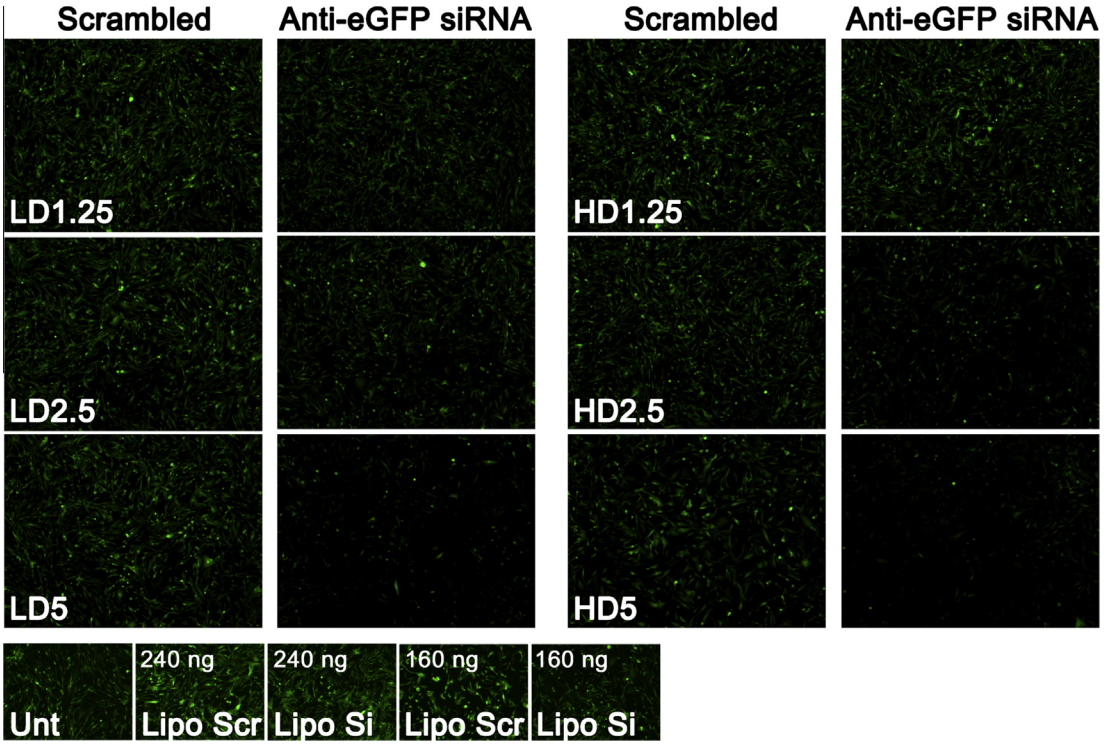

Fig. 5. Fluorescence microscope images of the eGFP channel showing GFP knockdown following transfection with various MAu/DNA/siRNA LbL nanoparticles; the Lipofectamine® 2000 conditions shown are 240 ng 0.5:1 and 160 ng 2.5:1 (200 ms eGFP exposure time; magnification of 5×; "scr" refers to scrambled siRNA and "si" refers to active anti-eGFP siRNA).

used as the middle polymer layer with two layers of DNA, the average layering efficiency decreased to 5.8 ± 0.5%. When nondegradable and highly charged PEI was used as the first and middle layers with two layers of DNA, the layering efficiency was similar to the single DNA layer efficiency, at 29 ± 1%. The nucleic acid layering efficiencies of DNA and siRNA for the co-delivery formulations were 12 ± 2 and 80 ± 3%, respectively. Further details on the quantification of layering efficiencies (Supplemental Experimental Section), the nucleic acid content contained in the supernatants washes (Fig. S4) and the nucleic acid adsorbed onto the plasticware during formulation (Fig. S5) are discussed in the Supplemental Information.

3.6. Polymer weight ratio

The 447 polymer w/ws for the LbL formulations are listed in Table 1 and Table S1. The DNA and siRNA co-delivery formulations were assessed at two different dosages and three different concentrations of the outer polymer layer (1.25, 2.5 and 5 mg ml^{-1} of 447). The siRNA-free, "DNA only" LbL formulations had a w/w that ranged from 0 to 92. The 447 w/w for the DNA and siRNA co-delivery formulations ranged from 14 to 83 w/w for DNA and from 17 to 104 w/w for siRNA. The degree to which the inner ionically complexed layer of polymer could contribute to the w/w was investigated using the PEI layer and was determined to range from 6 to 9 and from 8 to 12 w/w for DNA and siRNA, respectively, according to the OPA assay.

3.7. Transfection and cytotoxicity

3.7.1. siRNA-mediated knockdown

The SiRNA-mediated knockdown over time in human brain cancer cells was obtained by measuring the decreased endogenous GFP expression of GFP-positive human brain cancer cells following transfection with LbL particles containing GFP siRNA (Fig. 3). The maximum knockdown during the time course for each co-delivery formulation occurred on days 5 and 6, and was highest with MAu-P-D-SS37-siRNA-447 LD5 and HD5, the formulations with the greatest concentration of polymer 447 as the outside layer of the particles. The relative fluorescence over time was measured by fluorimetry on a plate reader and the fluorescence of individual cells was measured by flow cytometry at 7 days. There were no significant differences between the maximum and day 7, which was when flow cytometry was performed on all formulations ($p > 0.05$).

The knockdown varied according to the siRNA dosage and w/w, ranging from near 0 to 44 ± 5% according to the plate reader by measuring the average fluorescence (Fig. 3) and from near 0 to 34 ± 3% by flow cytometry (Fig. 4). RMA or normalized viability (to the untreated group) ranged from 73 ± 4 to 91 ± 6% among the layered NP formulations.

Lipofectamine® 2000, a commercially available leading non-viral transfection reagent, was used as a positive control at the same dosages as the co-delivery LD and HD formulations. According to the plate reader and flow cytometry assessment, the strongest knockdown observed with Lipofectamine® 2000 was with volume to siRNA mass ratios (μl:μg) of 0.5:1 and 2.5:1, with siRNA dosages of 240 and 160 ng, respectively. The 240 (0.5:1) and 160 ng (2.5:1) dosages reached their maximum knockdown on days 6 and 7, respectively (Fig. S6). According to the flow cytometer and the plate reader, the 240 ng dosage reached 20 ± 2 and 25 ± 7% knockdown, respectively, and the 160 ng dosage reached 6 ± 3 and 19 ± 5% knockdown, respectively, with the human brain cancer cells (Figs. S6 and S7). The 160 ng 2.5:1 Lipofectamine® 2000 condition was quite toxic, with an RMA of 44 ± 1%, whereas the 240 ng 0.5:1 was 90 ± 2% (Fig. S7). Fig. S6 shows all the knockdown time courses of Lipofectamine® 2000 positive controls tested at various dosages and ratios to siRNA with RMAs greater than 70% according to the CellTiter assay.

Fluorescence microscope images of the eGFP channel showing the strength of knockdown at day 7 from the co-delivery DNA and siRNA LbL formulations with varying dosages and w/w, as well as Lipofectamine® 2000 at 240 ng (0.5:1) and 160 ng (2.5:1) as positive controls, are shown in Fig. 5.

3.7.2. DNA-mediated expression

The exogenous DNA expression of the co-delivery DNA and siRNA LbL formulation reached maximal expression on day 2, so day 2 was chosen as the time to assess expression efficacy for all formulations in the study [24,29]. The expression of each of the co-delivery LbL formulation dosages at various w/w are shown in fluorescence micrograph images (Fig. 6). The expression ranged from near 0 to 10.8 ± 0.5% (Fig. 7). There was no statistical difference in the expression efficacy as measured by the percentage of positively transfected cells between HD5 and Lipofectamine® 2000 at a 100 ng dosage (2.5 μl:1 μg DNA). The RMA ranged from 73 ± 4 to 91 ± 6%.

The fluorescence images of the expression at day 2 of other non-siRNA containing LbL formulations, as well as their quantified expression according to flow cytometry, are shown in Figs. S8 and S9, respectively. The expression for the DNA only layered formulations ranged from near 0 to 37 ± 2%. The MAu-P-D-P formulation was associated with approximately 3% transfection and an RMA of 26 ± 2%, which was the most cytotoxic layered formulation investigated. The layered NP formulation that delivered two nucleic acid layers of DNA (no siRNA) that resulted in the highest transfection (28 ± 1%) was MAu-P-D-SS37-D-447. This is the same formulation of polymer layers chosen to co-deliver DNA and siRNA, and was associated with a high RMA of 91 ± 2%. Lipofectamine® 2000 at a dosage of 100 ng (2.5 μl:1 μg DNA) was associated with a transfection of 14 ± 2% and an RMA of 72 ± 5%. The formulations MAu-P-D-447, MAu-P-D-SS37-D-447 and MAu-P-D-447-D-447 were statistically significantly higher ($p < 0.0001$) than the Lipofectamine® 2000 positive control for exogenous DNA expression, at 2.6-, 2.0- and 1.6-fold, respectively (Fig. S9).

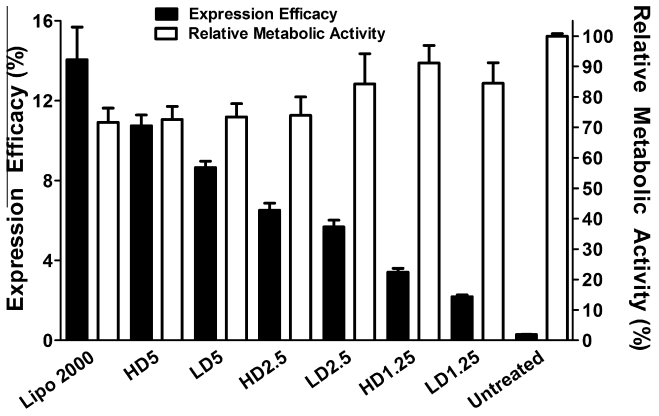

Fig. 7. DNA transfection efficacy and relative metabolic activity of MAu/DNA/siRNA LbL nanoparticles. Lipofectamine® 2000 was added at a 100 ng (2.5:1) dosage and is not statistically different from nanoparticle formulation HD5. Lipofectamine® 2000's expression was statistically significantly greater than all other formulations ($p < 0.0001$).

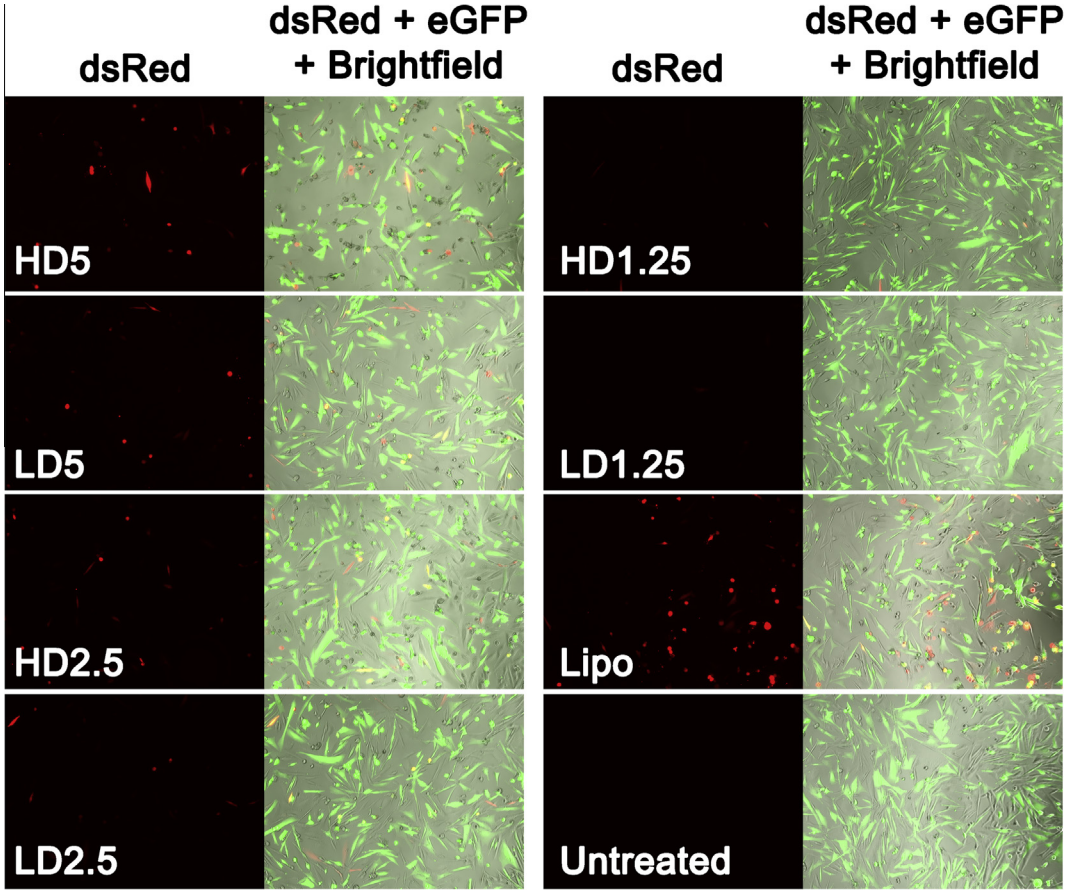

Fig. 6. Fluorescence microscope images showing exogenous dsRed expression following transfection of MAu/DNA/siRNA LbL nanoparticles. Lipofectamine® 2000 was added at a 100 ng dosage 2.5 μl:1 μg dsRed DNA; (200 ms eGFP and 600 ms dsRed exposure time; magnification of 10×).

3.7.3. Cytotoxicity of the co-delivery HD5 formulation 18 h post-degradation

The HD5 formulation which had undergone 18 h of degradation was statistically similar ($p = 0.34$) to the non-degraded formulation in terms of its relative metabolic activity (cytotoxicity).

3.8. Cellular uptake

Cellular uptake of the co-delivered LbL formulation HD5 is shown in Fig. 8 as measured by TEM. Panels A and B show particles on the order of ~200 nm. Panel C shows putative endosomes (far two left arrows) containing multiple aggregates of AuNPs in the endosome.

4. Discussion

4.1. CAu and MAu physical characterization

The tendency for MAu to aggregate less throughout the layering process indicates that MAu was superior for layering purposes in comparison to CAu. The differences in the UV–Vis spectra in Fig. S2 also further validate that the 11-MUA conjugation was successful.

4.2. Polymer characterization via gel permeation chromatography

SS37 is a disulfide-containing poly(amido amine) that was chosen as a degradable polyelectrolyte for layering because: (i) it is cationic, thus allowing nucleic acid complexation; (ii) it contains tertiary amines, which contribute to the proton sponge effect and endosomal escape [30]; and (iii) it contains disulfide linkages, which facilitate triggered degradation following cytoplasmic delivery as the cytosol is a reducing environment. The 447 PBAE was chosen as a degradable polyelectrolyte for layering as: (i) it is also cationic; (ii) it contains tertiary amines, which aid in the proton sponge effect and endosomal escape [30]; and (iii) it degrades hydrolytically due to its ester groups [31].

When we evaluated two layers of PEI coating AuNPs without using biodegradable polymers, we found the system to be less effective and excessively toxic (see Section 4.5.2) compared to LbL AuNPs with less PEI that utilized biodegradable polymers. This finding is in agreement with previous literature, which has shown that PBAE polyplexes, such as 447/DNA polyplexes that have polymer 447 on their surface, have improved cellular uptake and are more effective than PEI/DNA polyplexes for gene delivery [32–34]. We believe this same phenomenon makes 447 better than PEI as an outer layer on our particles. Further variation of the degradability of the polymers that make up the multilayers may be useful for controlling expression and knockdown over time.

4.3. Diameter and ZP

The NanoSight NS500 is able to directly measure the number-averaged NP diameter by Nanoparticle Tracking Analysis (NTA), rather than intensity-averaged NP diameter, like DLS in aqueous medium. In our testing, the uncoated CAu and MAu were unable to be accurately measured by NTA as the particle sizing limitation of the NanoSight NS500 with these materials was near 40 nm. However, for particles larger than 40 nm, the NanoSight measurements were similar to DLS measurements when measuring polyplexes or AuNPs layered with polymer. For example, DLS reported the diameters for MAu-P to be 80 ± 10 nm, which is near the NanoSight measurement of 113 ± 3 nm (errors are standard deviation; $n = 6$). Based on the TEM images (Fig. 1) and the DLS particle size data (Fig. 2), most MAu-P were singlets that had a PEI layer thickness of approximately 30 nm.

We hypothesize that the clustering effect during the layering process of positively charged polymer-coated AuNPs is due to multivalent interactions with DNA, as DNA is a large, anionic biomolecule. As the layering process proceeded, the NPs with outermost layers of SS37, siRNA and 447 were all relatively similar in diameter to the DNA layer, at approximately 200 nm. Assuming that no MAu was lost throughout the layering process, this would suggest that there are 43 ± 9 MAu cores per layered NP (the initial number of MAu nanoparticles divided by the final number of LbL particles based on NTA). Because of the 3-D aggregation of the MAu, it is difficult to count individual MAu in the final LbL nanoparticles by TEM directly (Fig. 1, far right). Assuming the highest possible density of packing by the 17 nm MAu in a packed regular lattice to be 0.74, the maximum theoretical number of MAu that could fit into the volume of a 200 nm diameter spherical NP would be approximately 1200. Because we estimate that there are approximately 43 MAu, rather than 1200, in an LbL NP, this finding suggests that approximately 4% of the occupied volume is MAu.

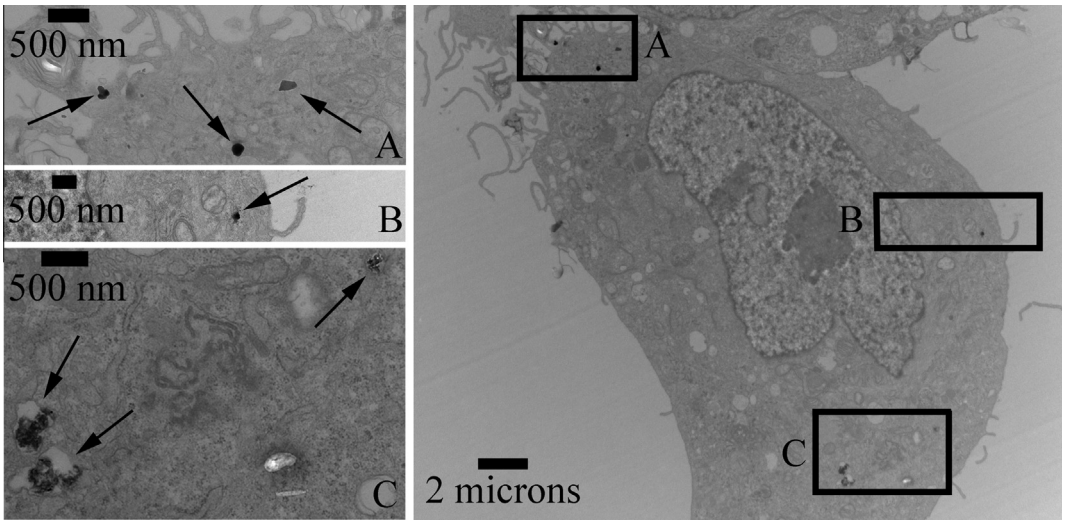

Fig. 8. TEM of MAu/DNA/siRNA LbL nanoparticles of formulation HD5 in GBM319 cells. (A and B) Particles that are ~200 nm. (C) Two left arrows indicate putative endosomes with multiple gold nanoparticle aggregates.

The reversal of the ZP demonstrates successful ionic complexation of each subsequent layer as the LbL coatings were built. The TEM agreed well with the NanoSight measurements in that the largest increase in diameter occurred at the DNA layer and that the layered particles reached approximately 200 nm in size.

The inclusion of PEG-conjugated 447 as the last layer could perhaps further optimize the system and minimize clearance by the reticulo-endothelial system [35]. Furthermore, hyaluronic acid could be another polyelectrolyte candidate to help control biodistribution [36].

4.4. Nucleic acid loading and layering efficiency

PEI was demonstrated to be more efficient at binding nucleic acid than the degradable and less positively charged polymer 447. On a mass basis, the siRNA had a higher loading efficiency into the LbL NPs than the DNA did (Fig. S4). The packing densities for the HD5 formulation by volume for DNA and siRNA were approximately 3×10^{-4} and 5×10^{-2} molecules per nm^3, respectively (the mass per particle was calculated using the particle concentration determined by NTA). Figs. S4 and S5 demonstrate that the two washing steps during the layering process are sufficient to ensure the removal of free polyelectrolyte from solution prior to the addition of subsequent polyelectrolyte layers to the particles. Previous work by our group has shown that it is possible to lyophilize PBAE/DNA polyplexes in the presence of a cryoprotectant, such as sucrose, resulting in the ability to store the gene delivery formulations long-term (>2 years) without compromising transfection efficacy [37].

4.5. Transfection and cytotoxicity

4.5.1. SiRNA-mediated knockdown

The w/w values in large part determined the time course of the knockdown; as the w/w increased for either 160 ng (LD) or 240 ng (HD) dosages, the knockdown increased in all cases. A decreased siRNA dosage did not necessarily result in decreased knockdown, depending on the w/w. The knockdown of the LD5 and HD5 formulations were statistically significantly higher than Lipofectamine® 2000 at 160 ng 2.5:1, by 1.4- and 1.8-fold, respectively, whereas formulations HD2.5, LD5 and HD5 were statistically significantly higher than Lipofectamine® 2000 at 240 ng 0.5:1 (Fig. 4), by 5.8-, 4.7- and 2.3-fold, respectively. The trends observed in the qualitative images are also in agreement with the assessments of knockdown from the fluorescence plate reader and the flow cytometer.

4.5.2. DNA-mediated expression

The expression of the co-delivery HD and LD formulations increased with increasing dosage and w/w. Generally, the RMA increased as the expression efficacy decreased. The most efficacious NP formulation for expression of DNA was MAu-P-D-447. The biodegradable polymer 447 was demonstrated to be superior to the conventionally used nondegradable polymer, PEI, as an outer layer. It was necessary to have an outer layer of 447 polymer as the last layer in light of MAu-P-D-P's results as well as the observation that MAu-P-D (0 w/w) was associated with very low transfection (0.12 ± 0.07%). MAu-P-D's results suggest that the inner layer of PEI alone was insufficient to promote transcription and translation and did not contribute substantially to toxicity.

4.5.3. Cytotoxicity of the co-delivery HD5 formulation 18 h post-degradation

The relative metabolic activities of the degraded and freshly prepared, non-degraded HD5 formulations were similar. Neither of these conditions showed significant cytotoxicity in GBM319 cells.

4.6. Cellular uptake

One of the advantages of using gold as the core of the NPs is that it can be tracked by imaging. The hybrid LbL particles were able to enter the cells, be tracked by TEM, release siRNA into the cytoplasm to achieve knockdown and release DNA that reaches the nucleus for exogenous expression. In contrast to viruses where a multiplicity of infection of even 1 can result in transduction, non-viral methods are less efficient and therefore require a much higher effective multiplicity of infection to get sufficient number of plasmids within the cell for sufficient expression, as just a few particles are observed to be within the cell in Fig. 8. However, further studies would need to be conducted to correlate the number of particles taken up with the resulting expression or knockdown.

5. Conclusions

We have successfully demonstrated that we can layer siRNA and DNA for co-delivery on AuNPs using polymers which degrade through different mechanisms. We found that the ZP reverses upon the addition of each oppositely charged layer of polyelectrolytes and the diameter reaches approximately 200 nm in size. PEI was found to be the most efficient polymer for loading nucleic acid, and polymer 447 was the most effective outer layer polymer for gene delivery. The gene knockdown achieved with the HD5 and LD5 formulations was superior to that achieved with optimized Lipofectamine® 2000 at comparable dosages in human brain cancer cells. These formulations also enabled exogenous DNA expression and intracellular tracking of the AuNPs by TEM. These LbL formulations are an enabling theranostic technology that can deliver combinations of genetic therapies along with an agent for potential imaging and photothermal therapy.

Acknowledgements

This work was supported by the National Institutes of Health (1R01EB016721). We would like to acknowledge the Microscope Facility at JHU for allowing usage of their facility, and the National Science Foundation Graduate Research Fellowships given to CJB (DGE-0707427) and SYT (DGE-1232825).

Appendix A. Figures with essential colour discrimination

Certain figures in this article, particularly Figs. 3, 5, 6 and Scheme 1, are difficult to interpret in black and white. The full colour images can be found in the on-line version, at http://dx.doi.org/10.1016/j.actbio.2014.09.020.

Appendix B. Supplementary data

Supplementary data associated with this article can be found, in the online version, at http://dx.doi.org/10.1016/j.actbio.2014.09.020.

References

[1] Frens G. Controlled nucleation for regulation of particle-size in monodisperse gold suspensions. Nat Phys Sci 1973;241:20–2.
[2] Pissuwan D, Niidome T, Cortie MB. The forthcoming applications of gold nanoparticles in drug and gene delivery systems. J Control Release 2011;149:65–71.
[3] Qian W, Curry T, Che Y, Kopelman R. Targeted delivery of peptide-conjugated biocompatible gold nanoparticles into cancer cell nucleus. In: Colloidal nanocrystals for biomedical applications Viii 2013;8595.
[4] Hainfeld JF, O'Connor MJ, Dilmanian FA, Slatkin DN, Adams DJ, Smilowitz HM. Micro-CT enables microlocalisation and quantification of Her2-targeted gold nanoparticles within tumour regions. Br J Radiol 2011;84:526–33.
[5] Park C, Youn H, Kim H, Noh T, Kook YH, Oh ET, et al. Cyclodextrin-covered gold nanoparticles for targeted delivery of an anti-cancer drug. J Mater Chem 2009;19:2310–5.

[6] Peng C, Qin JB, Zhou BQ, Chen Q, Shen MW, Zhu MF, et al. Targeted tumor CT imaging using folic acid-modified PEGylated dendrimer-entrapped gold nanoparticles. Polym Chem 2013;4:4412–24.
[7] Chawla JS, Amiji MM. Cellular uptake and concentrations of tamoxifen upon administration in poly(epsilon-caprolactone) nanoparticles. AAPS PharmSci 2003;5.
[8] Bae YH, Park K. Targeted drug delivery to tumors: myths, reality and possibility. J Control Release 2011;153:198–205.
[9] Wang TY, Halaney D, Ho D, Feldman MD, Milner TE. Two-photon luminescence properties of gold nanorods. Biomed Opt Express 2013;4:584–95.
[10] Yuan H, Register JK, Wang HN, Fales AM, Liu Y, Tuan VD. Plasmonic nanoprobes for intracellular sensing and imaging. Anal Bioanal Chem 2013;405:6165–80.
[11] Zhang Q, Iwakuma N, Sharma P, Moudgil BM, Wu C, McNeill J, et al. Gold nanoparticles as a contrast agent for in vivo tumor imaging with photoacoustic tomography. Nanotechnology 2009;20:395102.
[12] Huang XH, Jain PK, El-Sayed IH, El-Sayed MA. Plasmonic photothermal therapy (PPTT) using gold nanoparticles. Lasers Med Sci 2008;23:217–28.
[13] Loo C, Lowery A, Halas N, West J, Drezek R. Immunotargeted nanoshells for integrated cancer imaging and therapy. Nano Lett 2005;5:709–11.
[14] Jang H, Ryoo SR, Kostarelos K, Han SW, Min DH. The effective nuclear delivery of doxorubicin from dextran-coated gold nanoparticles larger than nuclear pores. Biomaterials 2013;34:3503–10.
[15] Elbakry A, Wurster EC, Zaky A, Liebl R, Schindler E, Bauer-Kreisel P, et al. Layer-by-layer coated gold nanoparticles: size-dependent delivery of DNA into cells. Small 2012;8:3847–56.
[16] Lee JS, Green JJ, Love KT, Sunshine J, Langer R, Anderson DG. Gold, poly(beta-amino ester) nanoparticles for small interfering RNA delivery. Nano Lett 2009;9:2402–6.
[17] Blacklock J, Mao GZ, Oupicky D, Mohwald H. DNA release dynamics from bioreducible layer-by-layer films. Langmuir 2010;26:8597–605.
[18] Elbakry A, Zaky A, Liebkl R, Rachel R, Goepferich A, Breunig M. Layer-by-layer assembled gold nanoparticles for siRNA delivery. Nano Lett 2009;9:2059–64.
[19] Flessner RM, Jewell CM, Anderson DG, Lynn DM. Degradable polyelectrolyte multilayers that promote the release of siRNA. Langmuir 2011;27:7868–76.
[20] Flessner RM, Yu Y, Lynn DM. Rapid release of plasmid DNA from polyelectrolyte multilayers: a weak poly(acid) approach. Chem Commun 2011;47:550–2.
[21] Saurer EM, Flessner RM, Sullivan SP, Prausnitz MR, Lynn DM. Layer-by-layer assembly of DNA- and protein-containing films on microneedles for drug delivery to the skin. Biomacromolecules 2010;11:3136–43.
[22] Lee SK, Han MS, Asokan S, Tung CH. Effective gene silencing by multilayered siRNA-coated gold nanoparticles. Small 2011;7:364–70.
[23] Sunshine JC, Bishop CJ, Green JJ. Advances in polymeric and inorganic vectors for nonviral nucleic acid delivery. Ther Deliv 2011;2:493–521.
[24] Bishop CJ, Ketola TM, Tzeng SY, Sunshine JC, Urtti A, Lemmetyinen H, et al. The effect and role of carbon atoms in poly(beta-amino ester)s for DNA binding and gene delivery. J Am Chem Soc 2013;135:6951–7.
[25] Tzeng SY, Guerrero-Cazares H, Martinez EE, Sunshine JC, Quinones-Hinojosa A, Green JJ. Non-viral gene delivery nanoparticles based on poly(beta-amino esters) for treatment of glioblastoma. Biomaterials 2011;32:5402–10.
[26] Zhao YH, Zhang Y, Yang Z, Li A, Dong JL. Simultaneous knockdown of BRAF and expression of INK4A in melanoma cells leads to potent growth inhibition and apoptosis. Biochem Biophys Res Commun 2008;370:509–13.
[27] Kang HC, Bae YH. Co-delivery of small interfering RNA and plasmid DNA using a polymeric vector incorporating endosomolytic oligomeric sulfonamide. Biomaterials 2011;32:4914–24.
[28] Ketola TM, Hanzlikova M, Leppanen L, Ravina M, Bishop CJ, Green JJ, et al. Independent versus cooperative binding in polyethylenimine–DNA and poly(L-lysine)–DNA polyplexes. J Phys Chem B 2013;117:10405–13.
[29] Eltoukhy AA, Siegwart DJ, Alabi CA, Rajan JS, Langer R, Anderson DG. Effect of molecular weight of amine end-modified poly(beta-amino ester)s on gene delivery efficiency and toxicity. Biomaterials 2012;33:3594–603.
[30] Boussif O, Lezoualc'h F, Zanta MA, Mergny MD, Scherman D, Demeneix B, et al. A versatile vector for gene and oligonucleotide transfer into cells in culture and in vivo: polyethylenimine. Proc Natl Acad Sci USA 1995;92:7297–301.
[31] Sunshine JC, Peng DY, Green JJ. Uptake and transfection with polymeric nanoparticles are dependent on polymer end-group structure, but largely independent of nanoparticle physical and chemical properties. Mol Pharm 2012;9:3375–83.
[32] Tzeng SY, Higgins LJ, Pomper MG, Green JJ. Student award winner in the Ph.D. category for the, society for biomaterials annual meeting and exposition, April 10–13, 2013, Boston, Massachusetts: biomaterial-mediated cancer-specific DNA delivery to liver cell cultures using synthetic poly(beta-amino ester)s. J Biomed Mater Res A 2013;2013(101):1837–45.
[33] Kim J, Sunshine JC, Green JJ. Differential polymer structure tunes mechanism of cellular uptake and transfection routes of poly(beta-amino ester) polyplexes in human breast cancer cells. Bioconjug Chem 2014;25:43–51.
[34] Bhise NS, Wahlin KJ, Zack DJ, Green JJ. Evaluating the potential of poly(beta-amino ester) nanoparticles for reprogramming human fibroblasts to become induced pluripotent stem cells. Int J Nanomed 2013;8:4641–58.
[35] Shmueli RB, Anderson DG, Green JJ. Electrostatic surface modifications to improve gene delivery. Expert Opin Drug Deliv 2010;7:535–50.
[36] Poon Z, Lee JB, Morton SW, Hammond PT. Controlling in vivo stability and biodistribution in electrostatically assembled nanoparticles for systemic delivery. Nano Lett 2011;11:2096–103.
[37] Guerrero-Cazares H, Tzeng SY, Young NP, Abutaleb AO, Quinones-Hinojosa A, Green JJ. Biodegradable polymeric nanoparticles show high efficacy and specificity at DNA delivery to human glioblastoma in vitro and in vivo. ACS Nano 2014;8:5141–53.
[38] Liu XO, Atwater M, Wang JH, Huo Q. Extinction coefficient of gold nanoparticles with different sizes and different capping ligands. Colloids Surf B 2007;58:3–7.
[39] Lin C, Blaauboer CJ, Timoneda MM, Lok MC, van Steenbergen M, Hennink WE, et al. Bioreducible poly(amido amine)s with oligoamine side chains: synthesis, characterization, and structural effects on gene delivery. J Control Release 2008;126:166–74.
[40] Lin C, Zhong ZY, Lok MC, Jiang XL, Hennink WE, Feijen J, et al. Linear poly(amido amine)s with secondary and tertiary amino groups and variable amounts of disulfide linkages: synthesis and in vitro gene transfer properties. J Control Release 2006;116:130–7.
[41] Lin C, Zhong ZY, Lok MC, Jiang XL, Hennink WE, Feijen J, et al. Novel bioreducible poly(amido amine)s for highly efficient gene delivery. Bioconjug Chem 2007;18:138–45.
[42] Tzeng SY, Green JJ. Subtle changes to polymer structure and degradation mechanism enable highly effective nanoparticles for siRNA and DNA delivery to human brain cancer. Adv Healthc Mater 2013;2:468–80.